Journal of
APPLIED
BIOMEDICINE

J Appl Biomed. **10**: 51–61, 2012
DOI 10.2478/v10136-011-0018-z
ISSN 1214-0287

ORIGINAL ARTICLE

Soman and VX: different effect on cellular signalling

Jaroslav Pejchal[1], Jan Österreicher[2], Jiří Kassa[3], Aleš Tichý[2], Zuzana Šinkorová[2], Lenka Zárybnická[2], Klára Kubelková[1], Kamil Kuča[1, 4]

[1]Center of Advanced Studies, [2]Department of Radiation Biology, [3]Department of Toxicology, Faculty of Military Health Sciences, University of Defence, Hradec Králové, Czech Republic
[4]Center for Biomedical Research, University Hospital Hradec Králové, Hradec Králové, Czech Republic

Received 16th May 2011.
Revised 26th July 2011.
Published online 10th November 2011.

Summary
The purpose of our study was to examine the early expression of p21 and activated transcription factors ATF-2, CREB, Elk-1, p53 after soman and VX poisoning, to throw light on the pathogenetic mechanism of nerve agent-induced non-specific effects. Male Wistar rats were i.m. poisoned by soman (60 $\mu g.kg^{-1}$ – 70% LD_{50}) or VX (8 $\mu g.kg^{-1}$ – 70% LD_{50}). Samples were taken 4, 24, and 72 hours after poisoning, immunohistochemically stained and phospho-ATF-$2^{Thr-69/71}$, phospho-$CREB^{Ser-133}$, phospho-Elk-$1^{Ser-383}$, phospho-$p53^{Ser-15}$, and protein p21 expressions were measured using computer Image analysis in apical and cryptal enterocytes of the colon transversum. After soman poisoning, we observed an increased phospho-CREB in cryptal enterocytes 4, 24, and 72 h after poisoning, while apical enterocytes expressed increased phospho-CREB only 72 h after intoxication. Phospho-Elk-1 significantly dropped 4 and 24 h after soman poisoning in the cryptal compartment. Activation of ATF-2 and p53 and expression of p21 were not changed 4, 24, and 72 h after soman poisoning. VX poisoning did not change any of measured parameters. Soman and VX showed a different effect on cellular signalling. Soman seems to cause additional effects, which are not related to the basic mechanism of nerve agent-induced toxicity and which temporarily suppress promitotic pathways of proliferating cells and persist in cells during the differentiation process.

Key words: soman; VX; ATF-2; CREB, Elk-1; p21; p53; enterocyte; image analysis

INTRODUCTION

Nerve agents are highly toxic organophosphates representing potential threats to both the military and the civilian population. The basic mechanism of their toxicity is well known and lies in irreversible binding to and inactivation of acetylcholinesterase (AChE, EC 3.1.1.7), which is associated with the accumulation of acetylcholine at the synapses and overstimulation of the cholinergic nervous system (Marrs 1993). By contrast, less is known about nerve agent-induced non-specific effects including the influence on non-cholinergic neurotransmitter levels and especially oxidative stress interfering with cellular DNA metabolism and resulting in organophosphate genotoxicity and mutagenicity (Kassa et al. 2000, Klaidman et al. 2003, Bajgar 2004). Oxidative stress and long-term alteration of DNA are considered to

✉ Kamil Kuča, Center of Advanced Studies, Faculty of Military Health Sciences, University of Defence, Třebešská 1575, 500 01 Hradec Králové, Czech Republic
kucakam@pmfhk.cz
☎ +420 973 253 028; +420 724 692 608
+420 495 513 018

contribute to the long-term toxic effects of nerve agents (Pazdernik et al. 2001, Klaidman et al. 2003). Therefore, finding the mechanisms of nerve agent-induced non-specific effects might contribute to early diagnosis and complex treatment of nerve agent poisoning.

Oxidative stress causes generalized damage to all molecular components (DNA, proteins, lipids) and even gives rise to the most deleterious form of cellular lesion, called double strand breaks (DSB) (Steinboeck et al. 2010). Eukaryotic cells respond to oxidative stress and/or DNA damage by activating multiple signal transduction pathways to maximize cellular survival while minimizing the chance of carcinogenesis (Takekawa et al. 2000). The most important signalling pathways related to oxidative stress and/or DNA damage are pathways related to protein p53 and mitogen-activated protein kinase (MAPK) pathways (Giaccia et al. 1998, Kyriakis and Avruch 2001).

The protein p53 is a transcription factor whose function is regulated through phosphorylation at multiple sites by different kinases (Kyriakis and Avruch 2001). The presence of DSB induces phosphorylation of p53 at serine 15 by DNA-dependent protein kinase (DNA-PK) and ataxia telangiectasia mutated kinase (ATM). Both kinases are at the top of the DNA damage signalling network and play a key role in the response of p53 to DNA damage (Lakin and Johnson 1999). Phosphorylation of p53 at serine 15 modulates its stability and sequence-specific DNA binding activity leading to transcription of several p53 targets, including the cyclin-dependent kinase inhibitor p21 (el-Deiry et al. 1993, Wittlinger et al. 2007). Protein p21 blocks the cell cycle which allows the cells to assess the extent of DNA damage and initiate repair or to trigger an apoptotic response (Jung et al. 2010).

In contrast to DNA damage specific phosphorylation of p53 at serine 15, MAPK signalling pathways are activated in response to many different stimuli such as γ-radiation, UV radiation, DNA damaging reagents, osmotic shock, and oxidant stressors (Johnson and Lapadat 2002). So far, three main groups of MAPK cascades have been identified: ERK (extracellular signal-regulated kinase) pathway, preferably activated by mitogenic stimuli, p38 and JNK (c-Jun N-terminal kinase) pathways regulated by environmental stressors. These cascades modulate the function of a very wide range of transcription factors, including Elk-1, ATF-2, CREB, through which MAPK pathways adjust cellular transcription phenotype to the new conditions – to the presence of damage and/or stress stimulation (Kyriakis and Avruch 2001).

To evaluate the effects of nerve agents on cellular signalling, we investigated the impact of soman and the VX agent on phosphorylation of p53 at serine 15, the expression of protein p21 and activation of MAPK-related transcription factors Elk-1, ATF-2, and CREB *in vivo*. Because of the different penetration of both nerve agents through the blood-brain barrier (Bajgar et al. 2010), a model of rat colon enterocytes was chosen for the study.

MATERIAL AND METHODS

Animals

Male Wistar rats aged 12–16 weeks and weighing 250–300 g (Navel, Konárovice, Czech Republic) were kept in an air-conditioned room (22±2 °C and 50±10% relative humidity, with lights from 7.00 to 19.00 hours) and allowed access to standard food and tap water *ad libitum*. Before the start of the experiment (soman, VX, or saline administration), animals spent 15 days of acclimatization in the laboratory vivarium. Handling of the experimental animals was done under the supervision of the Ethics Committee of the Faculty of Military Health Sciences in Hradec Králové (Czech Republic).

Chemicals

Soman (GD; pinacolyl methylphosphonofluoridate) and the VX agent [O-ethyl S-(2-isopropyl-aminoethyl) methyl phosphonothioate] were obtained from the Military Technical Institute in Brno (Czech Republic). Their purity (97–98%) was assayed by acidimetric titration. All other drugs and chemicals of analytical grade were obtained commercially and used without further purification. Soman, the VX agent and saline were administered intramuscularly (i.m.) at a volume of 1 ml/kg of body weight (b.w.).

Procedure

Soman experiment

Saline was administered i. m. to twenty-four control rats divided into three groups and all of them were killed by cervical dislocation 4, 24 and 72 hours after saline administration, respectively. Soman was administered i. m. at a dose of 60 μg/kg (70% LD_{50}), to twenty-four experimental rats who were then divided into three groups, all of which were killed by cervical dislocation 4, 24 and 72 hours after the poisoning, respectively.

VX experiment

Saline was administered i.m. to twenty-four control rats who were then divided into three groups all of

which were killed by cervical dislocation 4, 24 and 72 hours after saline administration, respectively. The VX agent was administered i. m. to thirty experimental rats at a dose 8 μg/kg (70% LD_{50}); they were divided into three groups, all of which were killed by cervical dislocation 4, 24 and 72 hours after VX poisoning, respectively.

Histological examination

The central part of the *colon transversum* was removed from the rats and carefully fixed with a 10% neutral buffered formalin (Chemapol, Prague, Czech Republic). Samples were subsequently embedded into paraffin (Paramix, Holice, Czech Republic), 5 μm thick tissue sections were cut and immuno-histochemical detection of ATF-2 phosphorylation at threonine 69 and 71, CREB phosphorylation at serine 133, Elk-1 phosphorylation at serine 383, p53 phosphorylation at serine 15, and protein p21 was performed with a standard peroxidase technique. After blocking of the endogenous peroxidase activity for 20 min [1.8 ml of 30% hydrogen peroxide (Vitrum, Prague, Czech Republic) in 100 ml methanol (Kulich, Hradec Králové, Czech Republic)], the tissue sections were incubated for 1 hour with antibodies: rabbit polyclonal anti-phospho-ATF-$2^{Thr-69/71}$ diluted 1:50; rabbit monoclonal anti-phospho-$CREB^{Ser-133}$ diluted 1:100; mouse monoclonal anti-Elk-$1^{Ser-383}$ diluted 1:100 (all from Biotech, Prague, Czech Republic); rabbit polyclonal-anti-$p53^{Ser-15}$ diluted 1:100 (Merck, Říčany, Czech Republic), and mouse monoclonal anti-p21 diluted 1:50 (ITA-interact, Prague, Czech Republic) in phosphate buffered saline (PBS, Sigma-Aldrich, Prague, Czech Republic) pH 7.2 and were then washed three times in PBS. All slides were then incubated for 20 min with secondary antibodies. A ready-to-use biotinylated anti-rabbit secondary antibody (DakoCytomation, Prague, Czech Republic) was used for the slides previously incubated with rabbit primary antibodies and biotin-SP-conjugated AffiniPure donkey anti-mouse secondary antibody diluted 1:500 (Spinchem, Plzeň, Czech Republic) was used for slides previously incubated with mouse primary antibodies. The excess of secondary antibodies was then washed off with PBS. Subsequently, all slides were incubated with streptavidin horseradish peroxidase (Dako Cytomation, Prague, Czech Republic) under the same conditions as the secondary antibody, washed with PBS and finally, 0.05% 3,3´-diaminobenzidi-netetrahydrochloride-chromogen solution (Sigma-Aldrich, Prague, Czech Republic) in PBS containing 0.02% hydrogen peroxide, was added for 10 min to visualize the antigen-antibody complex *in situ*.

Image analysis

Stained samples were evaluated using the BX-51 microscope (Olympus, Prague, Czech Republic) and computer image analysis ImagePro 5.1. (Media Cybernetics, Bethesda, USA). Ten microscopic fields at a 400fold original magnification were randomly selected from each rat sample. Image analysis was performed separately in two compartments – in apical enterocytes and in enterocytes of lateral sides of crypts in the area of 2250 μm^2 representing 30–40 cells per field and compartment. The immuno-reactive structures of inverted RGB scale were detected in the range: red 56-255, green 76-255, and blue 94-255, where 0 is white and 255 is the colour black. Subsequently, integral optical density (IOD) of viewing fields was measured. The IOD parameter reflects the intensity of positivity within the detected area. The scale represents levels from 0 to 2×10^5 for the detected area.

Histopathological evaluation of staining intensity

The samples were examined in a "blind" manner by two independent observers. The level of staining was estimated semiquantitatively by using the immunoreactive score (IRS) (Remmele and Stegner 1987). The IRS is calculated by multiplying the staining intensity (graded between 0 and 3) and the percentage of positive cells (graded between 0 and 4: 0, negative; 1, 1–10%; 2, 11–50%; 3, 51–80%; 4, 81–100%). It allows a maximum value of 12. On the basis of IRS, the staining pattern was defined as: negative (IRS: 0), weak (IRS: 1–4), moderate (IRS: 5–8), and strong (IRS: 9–12).

Statistical analysis

The Mann-Whitney test was used for the statistical analysis giving mean ± 2 × S.E.M. (Standard error of mean). The differences were considered significant when $p \leq 0.05$.

RESULTS

Mortality and symptoms of nerve agent poisoning

After soman poisoning, 5 of 24 animals died prior to the time of sample collection (Table 1). This result is comparable to VX poisoning, in which 6 of 30 animals died prior to the time of sample collection (Table 2). Symptoms exhibited with soman and VX poisoning (salivation, chewing, generalised convulsions and/or convulsions in the forelimb or hindlimb) were present in all animals early after intoxication and disappeared within 24 hours after soman as well as VX poisoning.

Table 1. **Survival of rats following exposure to soman.**

Groups (time of sample collection)	Survival in the time of sample collection (survived/total)	Time of death (min)
Saline (4 hours)	8/8	
Saline (24 hours)	8/8	
Saline (72 hours)	8/8	
Soman (4 hours)	6/8	152, 180
Soman (24 hours)	6/8	200, overnight
Soman (72 hours)	7/8	181

Table 2. **Survival of rats following exposure to VX.**

Groups (time of sample collection)	Survival in the time of sample collection (survived/total)	Time of death (min)
Saline (4 hours)	8/8	
Saline (24 hours)	8/8	
Saline (72 hours)	8/8	
Soman (4 hours)	8/10	110, 130
Soman (24 hours)	8/10	156, overnight
Soman (72 hours)	8/10	62, overnight

Effect of nerve agents on activation of p53, Elk-1, CREB, ATF-2 and and expression of protein p21

Phospho-p53^{Ser-15}

In comparision with the control animals, we did not find any significant changes in phospho-p53^{Ser-15} levels 4, 24, and 72 hours after soman or VX poisoning (Table 3 and 8).

Expression of p21

Similarly to phospho-p53^{Ser-15}, p21 expression was not found to be significantly changed 4, 24, and 72 hours after soman or VX intoxication (Table 4 and 8).

Phospho-Elk-1$^{Ser-383}$

In comparison with the control animals, phospho-Elk-1$^{Ser-383}$ was significantly decreased in cryptal enterocytes 4 and 24 hours after soman intoxication. The IOD values decreased 2.7- and 1.6-fold, respectively. A significant change of Elk-1 activation was also measured oculometrically in crypts 4 hours after soman poisoning. On the other hand, VX poisoning did not change activation of Elk-1 compared to control values (Table 5 and 8).

Phospho-CREB$^{Ser-133}$

The level of phospho-CREB$^{Ser-133}$ in apical enterocytes was significantly increased 72 hours after soman administration (IOD increased 3.1-fold), while cryptal phospho-CREB levels were found to be significantly higher 4, 24, and 72 hours after soman intoxication with IOD values being 3.3-, 3.2-, and 1.7-fold increased, respectively. Significantly higher phospho-CREB$^{Ser-133}$ was measured oculometrically in apical enterocytes 72 hours after soman poisoning. VX poisoning did not change the activation of CREB in both compartments compared to control values (Table 6 and 8).

Phospho-ATF-2$^{Thr-69/71}$

No significantly different changes of phospho-ATF-2 levels were measured in rat colon enterocytes 4, 24, and 72 hours after soman or VX intoxication (table 7 and 8).

Table 3. **Average IOD values of phospho-p53^{Ser-15} per microscopic field ± 2 × S.E.M.**

	Integral optical density (IOD)		
time (h)	4	24	72
	apical enterocytes		
control	400±100	400±100	400±100
SOMAN	500±100	700±300	500±100
control	1900±900	3100±1400	3800±1500
VX	1200±600	3200±900	2800±1200
	cryptal enterocytes		
control	0±0	100±100	0±0
SOMAN	0±0	100±0	0±0
control	100±100	200±100	100±100
VX	0±0	100±100	100±100

Note: Although the same primary antibodies (same supplier, same catalogue number) were used for soman and VX experiments, their batches differed. Therefore, significant colour differences between soman and VX control groups can be found. See also table 6 and 7.

Table 4. **Average IOD values of protein p21 expression per microscopic field ± 2 × S.E.M.**

	Integral optical density (IOD)		
time (h)	4	24	72
	apical enterocytes		
control	900±300	2000±600	1700±1200
SOMAN	1000±300	2500±1300	1500±900
control	1400±500	1500±100	1300±700
VX	1100±500	1400±400	1000±500
	cryptal enterocytes		
control	100±0	100±0	100±100
SOMAN	0±0	200±100	0±0
control	100±100	100±100	100±100
VX	100±100	100±100	100±100

Table 5. **Average IOD values of phospho-Elk-1$^{Ser-383}$ per microscopic field ± 2 × S.E.M.**

	Integral optical density (IOD)		
time (h)	4	24	72
	apical enterocytes		
control	39500±6000	32400±6500	28600±3700
SOMAN	31600±3900	31300±7200	36800±6300
control	35600±5100	32600±3400	31700±4700
VX	34600±4300	35500±3500	37000±5000
	cryptal enterocytes		
control	36900±6400	28800±6100	30000±3700
SOMAN	13600±4200*	17500±5500*	22700±4200
control	32500±5800	31000±6000	25800±4500
VX	30600±5100	26700±3600	24600±3800

***** statistically significant as compared with control

Table 6. **Average IOD values of phospho-CREB$^{Ser-133}$ per microscopic field ± 2 × S.E.M.**

	Integral optical density (IOD)		
time (h)	4	24	72
	apical enterocytes		
control	700±100	1200±300	1400±700
SOMAN	900±200	2000±900	4300±2300*
control	2400±600	2500±900	3500±1100
VX	2900±800	3700±800	4500±2200
	cryptal enterocytes		
control	300±100	500±100	1300±600
SOMAN	1000±200*	1600±400*	2200±700*
control	1200±200	1100±300	1200±300
VX	1200±400	1600±500	900±200

symbols as in Table 5

Table 7. **Average IOD values of phospho-ATF-2$^{Thr-69/71}$ per microscopic field ± 2 × S.E.M.**

	Integral optical density (IOD)		
time (h)	4	24	72
	apical enterocytes		
control	300±200	500±100	400±200
SOMAN	400±200	700±200	500±100
control	1300±300	1600±600	2600±1000
VX	2000±1000	2800±1200	2000±700
	cryptal enterocytes		
control	200±100	300±100	600±200
SOMAN	300±100	300±100	700±200
control	2900±700	3000±900	2200±400
VX	2700±600	3100±1100	2700±600

Table 8. **Immunoreactive score of protein expression and protein activation after nerve agent poisoning ± 2 × S.E.M.**

		4 h	24 h	72 h	4 h	24 h	72 h
		apical enterocytes			cryptal enterocytes		
phospho-p53	control	1.6±0.5	2.1±0.7	1.6±0.6	0.0±0.0	0.0±0.0	0.0±0.0
	soman	2.2±0.4	1.8±0.5	2.6±0.8	0.0±0.0	0.0±0.0	0.0±0.0
	control	3.0±1.2	2.4±0.8	4.7±1.2	0.0±0.0	0.0±0.0	0.0±0.0
	VX	2.3±0.7	2.7±1.1	2.8±1.2	0.0±0.0	0.0±0.0	0.0±0.0
p21	control	3.9±0.9	4.4±1.5	3.3±1.0	0.0±0.0	0.0±0.0	0.0±0.0
	soman	4.0±1.0	4.1±1.5	4.3±1.4	0.0±0.0	0.0±0.0	0.0±0.0
	control	2.3±1.2	3.3±1.2	3.9±0.8	0.0±0.0	0.0±0.0	0.0±0.0
	VX	2.6±0.8	3.4±1.4	3.8±1.1	0.0±0.0	0.0±0.0	0.0±0.0
phospho-Elk-1	control	11.6±0.3	11.8±0.4	12.0±0.0	11.9±0.2	11.6±0.4	11.9±0.0
	soman	11.9±0.2	11.6±0.4	12.0±0.0	9.1±1.1*	11.0±0.3	11.3±0.5
	control	11.6±0.5	11.8±0.2	11.4±0.6	11.5±0.7	11.3±0.6	11.6±0.4
	VX	11.5±0.6	11.0±0.7	11.3±0.6	11.4±0.8	10.9±0.7	11.3±0.6
phospho-CREB	control	2.9±0.6	3.1±0.7	3.8±1.2	2.6±0.8	2.3±1.0	2.0±0.9
	soman	2.6±0.5	4.0±1.4	6.1±2.2*	3.7±0.8	4.8±1.2	2.4±0.9
	control	4.1±1.0	3.3±1.1	4.6±0.9	4.1±0.9	3.7±1.1	3.7±1.0
	VX	4.6±1.6	4.8±1.2	4.3±1.6	4.0±0.8	4.1±0.9	3.3±0.6
phospho-ATF-2	control	2.2±0.3	3.9±1.4	2.1±0.7	1.9±0.6	3.1±1.1	2.8±0.9
	soman	2.9±0.5	3.0±0.4	3.0±1.2	2.6±0.6	3.4±0.9	3.3±1.7
	control	1.8±0.4	1.9±0.8	3.4±0.7	3.6±0.6	3.4±1.1	3.1±0.5
	VX	2.4±1.6	2.5±0.6	2.2±1.0	3.2±0.7	3.1±0.4	3.2±0.7

symbols as in Table 5

DISCUSSION

The *in vivo* model of gastrointestinal epithelium provides a unique tool for assessing the effect of soman and VX poisoning on undifferentiated and proliferating cells localized at the base of the crypts and on differentiated cells at the inner intestinal surface. To evaluate the non-specific effects of nerve agents on rat enterocytes, we focused on two groups of proteins. The first group consists of two proteins – cell cycle cyclin-dependent kinase inhibitor p21 and its activated regulator p53, which is involved in the pathogenesis of soman-induced cerebral damage (Baille et al. 2005). The second group of proteins is formed by Elk-1, CREB, and ATF-2, which are regulated by MAPK signalling cascades. P38 MAPK pathway participates in the regulation of the soman response in the rat cerebelum (Pejchal et al. 2008, 2009).

The first group of proteins – p21 and activated p53 – did not show any significant changes after soman and VX poisoning. In the control as well as in the soman and VX poisoned animals, we observed slight p21 and phospho-p53^{Ser-15} positivity along apical enterocytes and negative p21 and phospho-p53^{Ser-15} expression in crypts. Both proteins play an important role in processes such as intestinal differentiation or regulation of intestinal homeostatis in response to strong oxidative stressors such as ionising radiation (Wilson et al. 1998, Tian and Quaroni 1999). According to our results, these processess do not seem to be affected by either nerve agent in rat intestinal cells. It is likely that neither nerve agent generates oxidative stress leading to activation of p53/p21 signalling in enterocytes. This is in contrast to Baille et al. (2005) who described soman-induced expression of p53 in cerebral tissue. Nevertheless, Baille et al. (2005) observed increased p53 expression in the nuclei of injured or dying cells which correlated with the duration of seizures and, therefore, the difference between their study and ours could be explained by the excitotoxicity of the neurones and a higher susceptibility of cerebral cells to hypoxia during convulsions (Morrison and Kinoshita 2000, Guo et al. 2008).

In comparison with p21 and phospho-p53 expression, MAPK-regulated transcription factors showed different activation patterns when the soman or VX agent was applied. According to our results, soman modulates the activation of Elk-1 and CREB, while both proteins are unaffected by the VX agent. The soman data are also supported by the findings from other laboratories that organophosphorus agents DFP and chlorpyrifos alter phosphorylation of CREB (Schuh et al. 2002, Damodaran et al. 2009). Since the symptoms of nerve agent intoxication were similarly expressed in both groups, it is likely that the effect of soman on Elk-1 and CREB activation is not related to the basic mechanism of nerve agent-induced acute toxicity (irreversible AChE inhibition). There are two possible explanations. Either the effect is concentration-dependent and the dose of VX was too low to affect Elk-1 and CREB activation or soman possesses an additional mechanism through which it modulates the biological outcome of poisoning.

As with the mechanism of the soman-induced non-specific effect, its biological outcome is uncertain. The transcription factor Elk-1 is a target of ERK1/2 kinase (Kyriakis and Avruch 2001). In enterocytes, ERK1/2 signalling supports cell survival and it is required for S-phase entry and proliferation (Rivard et al. 1999, Gauthier et al. 2001, Boucher et al. 2004), in which Elk-1 may participate via transcriptional regulation of growth stimulating factors such as cyclin D1 (Shin et al. 2003). In addition, *in vitro* experiments have shown that ERK inhibition induced by cell-cell contacts could be a critical step in initiating G_1 cell cycle arrest and induction of differentiation (Aliaga et al. 1999, Laprise et al. 2004). Interestingly, we observed a rather diffuse phospho-Elk-1 pattern in the crypts and compartmentalization of phospho-Elk-1 into the supranuclear cytoplasmatic space at the crypt-villus junction and superficial enterocytes (Figs 1 and 2) in both control and soman-poisoned animals. This suggests that the relocation of phospho-Elk-1 into the cytoplasm might be a regulatory mechanism contributing to cell cycle arrest, differentiation and maturation of enterocytes. Since soman poisoning does not affect the Elk-1 activation pattern in superficial enterocytes, the finding may support the fact that soman does not influence the enterocyte differentiation process based on p21 data. In contrast, decreased phosphorylation of Elk-1 in crypts measured 4 and 24 hours after the soman poisoning indicates that soman temporarily downregulates enterocyte proliferation at the regulatory protein level.

Phosphorylation of CREB at serine 133 is regulated by ERK and p38 kinase pathways and other kinases such as protein kinases A (Kyriakis and Avruch 2001). *In vitro* experiments conducted on enterocyte-derived cell lines implicate CREB in the regulation of cell differentiation as well as survival and proliferation (Paruchuri and Sjölander 2003, Lee et al. 2010). Low control levels of activated CREB may therefore maintain mitotic activity in crypts and the differentiation process in the apical compartment. Consequently, increased CREB phosphorylation observed 4 and 24 hours after soman poisoning might serve as a compensatory action for decreased Elk-1

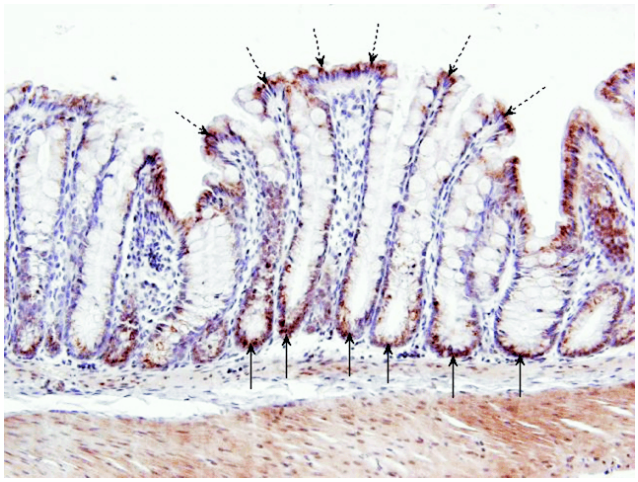

Fig. 1. **Sample of control (saline, 4 hours after administration) rat *colon transversum* with immunohistochemical detection of phospho-Elk-1$^{Ser-383}$ at 200-fold magnification.** In apical enterocytes (dashed arrows), phospho-Elk-1$^{Ser-383}$ assumed a supranuclear cytoplasmatic pattern, while in crypts (solid arrows), we observed a rather diffuse pattern. For publication purposes, samples were counterstained with Harris heamatoxylin.

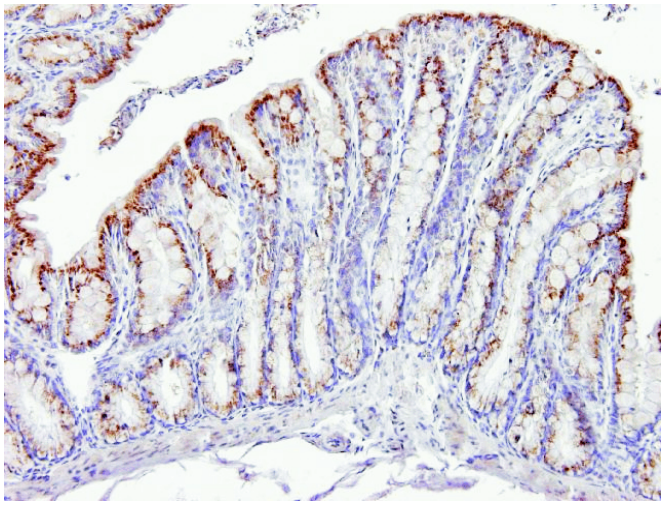

Fig. 2. **Sample of soman-poisoned (single dose of 70 % LD_{50}) rat *colon transversum* at 200-fold original magnification 4 hours after the poisoning.** Immunohistochemical detection did not show any change of phospho-Elk-1$^{Ser-383}$ pattern in apical enterocytes but we observed significantly decreased phospho-Elk-1$^{Ser-383}$ positivity in crypts. For publication purposes, samples were counterstained with Harris heamatoxylin.

activity in cryptal enterocytes. Nevertheless, this hypothesis does not explain the increased activation of CREB in both intestinal compartments 72 hours after soman intoxication. A more likely explanation associates the delayed CREB phosphorylation in crypts and its shift to apical enterocytes correlating with 3–5 day cycle of complete mucosal exchange (Laprise et al. 2004) with the presence of DNA damage. *In vitro*, soman is capable of rapid binding to DNA and interference with DNA metabolism (Ivanović et al. 1985, Klein et al. 1987). Thus, we argue that soman binds to DNA and forms DNA adducts *in vivo*. According to our results, the amount of DNA damage is not so extensive as to activate p53 and increase p21 expression but it seems to be sufficient enough to impair the DNA replication

process, which leads to downregulation of phospho-Elk-1 expression and activation of DNA repair mechanisms, in which CREB may participate via regulation of genes involved in the base and nucleotide excision repair systems (Grösch and Kaina 1999, Lemée et al. 2007).

It is also noteworthy that changes in MAPK signalling observed in rat colon transversum after soman poisoning precede the delayed alteration of MAPK cascades in the cerebellar tissue (Pejchal et al. 2008, 2009). Alteration of MAPK is associated with many neurodegenerative diseases (Miloso et al. 2008) and may play an important role in delayed toxicity of nerve agents in CNS (Pejchal et al. 2008, 2009). From this point of view, the detection of activated transcription factors in enterocytes early after soman poisoning may have a prognostic value. A disadvantage is the invasive nature required for accessing gut enterocytes. Therefore, blood or more accessible proliferating cell lines such as skin keratinocytes or epithelial cells from *cavum oris* should be used. However, this suggestion has to be verified by further experiments detecting the prognostic markers in other tissues.

ACKNOWLEDGEMENTS

We would like to thank Mrs. Šárka Průchová for her skillful technical assistance. This work was supported by the Ministry of Defence of the Czech Republic through grant MO0FVZ0000501 (institutional support No. 9079301306023) and grant OVUOFVZ200812 – RADSPEC.

REFERENCES

Aliaga JC, Deschênes C, Beaulieu JF, Calvo EL, Rivard N. Requirement of the MAP kinase cascade for cell cycle progression and differentiation of human intestinal cells. Am J Physiol. 277: 631–641, 1999.

Baille V, Clarke PG, Brochier G, Dorandeu F, Verna JM, Four E, Lallement G, Carpentier P. Soman-induced convulsions: the neuropathology revisited. Toxicology. 215: 1–24, 2005.

Bajgar J. Organophosphate/nerve agent poisoning: mechanism of action, diagnosis, prophylaxis, and treatment. Adv Clin Chem. 38: 151–216, 2004.

Bajgar J, Hajek P, Karasova Zdarova J, Kassa J, Paseka A, Slizova D, Krs O, Kuca K, Jun D, Fusek J, Capek L. A comparison of tabun-inhibited rat brain acetylcholinesterase reactivation by three oximes (HI-6, obidoxime, and K048) *in vivo* detected by biochemical and histochemical techniques. J Enzyme Inhib Med Chem. 25: 790–797, 2010.

Boucher MJ, Jean D, Vézina A, Rivard N. Dual role of MEK/ERK signaling in senescence and transformation of intestinal epithelial cells. Am J Physiol Gastrointest Liver Physiol. 286: 736–746, 2004.

Damodaran TV, Gupta RP, Attia MK, Abou-Donia MB. DFP initiated early alterations of PKA/p-CREB pathway and differential persistence of beta-tubulin subtypes in the CNS of hens contributes to OPIDN. Toxicol Appl Pharmacol. 240: 132–142, 2009.

el-Deiry WS, Tokino T, Velculescu VE, Levy DB, Parsons R, Trent JM, Lin D, Mercer WE, Kinzler KW, Vogelstein B. WAF1, a potential mediator of p53 tumor suppression. Cell. 75: 817–825, 1993.

Gauthier R, Harnois C, Drolet JF, Reed JC, Vézina A, Vachon PH. Human intestinal epithelial cell survival: differentiation state-specific control mechanisms. Am J Physiol Cell Physiol. 280: 1540–1554, 2001.

Giaccia AJ, Kastan MB. The complexity of p53 modulation: emerging patterns from divergent signals. Genes Dev. 12: 2973–2983, 1998.

Grösch S, Kaina B. Transcriptional activation of apurinic/apyrimidinic endonuclease (Ape, Ref-1) by oxidative stress requires CREB. Biochem Biophys Res Commun. 261: 859–863, 1999.

Guo Y, Korteweg C, McNutt MA, Gu J. Pathogenetic mechanisms of severe acute respiratory syndrome. Virus Res. 133: 4–12, 2008.

Ivanović V, Rapić V, Bosković B. Pinacolyl methylphosphonochloridate: *in vitro* covalent binding to DNA and mutagenicity in the Ames test. Mutat Res. 142: 9–12, 1985.

Johnson GL, Lapadat R. Mitogen-activated protein kinase pathways mediated by ERK, JNK, and p38 protein kinases. Science. 298: 1911–1912, 2002.

Jung YS, Qian Y, Chen X. Examination of the expanding pathways for the regulation of p21 expression and activity. Cell Signal. 22: 1003–1012, 2010.

Kassa J, Skopec F, Vachek J. The long term changes in liver DNA and total protein contents following low level sarin exposure in rats. Acta Medica (Hradec Králové). 43: 19–22, 2000.

Klaidman LK, Adams JD, Jr., Cross R, Pazdernik TL, Samson F. Alterations in brain glutathione homeostasis induced by the nerve gas soman. Neurotox Res. 5: 177–182, 2003.

Klein AK, Nasr ML, Goldman M. The effects of *in vitro* exposure to the neurotoxins sarin (GB) and soman (GD) on unscheduled DNA synthesis by rat hepatocytes. Toxicol Lett. 38: 239–249, 1987.

Kyriakis JM, Avruch J. Mammalian mitogen-activated protein kinase signal transduction pathways activated by stress and inflammation. Physiol Rev. 81: 807–869, 2001.

Lakin ND, Jackson SP. Regulation of p53 in response to DNA damage. Oncogene. 18: 7644–7655, 1999.

Laprise P, Langlois MJ, Boucher MJ, Jobin C, Rivard N. Down-regulation of MEK/ERK signaling by E-cadherin-dependent PI3K/Akt pathway in differentiating intestinal epithelial cells. J Cell Physiol. 199: 32–39, 2004.

Lee HY, Crawley S, Hokari R, Kwon S, Kim YS. Bile acid regulates MUC2 transcription in colon cancer cells via positive EGFR/PKC/Ras/ERK/CREB, PI3K/Akt/IkappaB/NF-kappaB and p38/MSK1/CREB pathways and negative JNK/c-Jun/AP-1 pathway. Int J Oncol. 36: 941–953, 2010.

Lemée F, Bavoux C, Pillaire MJ, Bieth A, Machado CR, Pena SD, Guimbaud R, Selves J, Hoffmann JS, Cazaux C. Characterization of promoter regulatory elements involved in downexpression of the DNA polymerase kappa in colorectal cancer. Oncogene. 26: 3387–3394, 2007.

Marrs TC. Organophosphate poisoning. Pharmacol Ther. 58: 51–66, 1993.

Miloso M, Scuteri A, Foudah D, Tredici G. MAPKs as mediators of cell fate determination: an approach to neurodegenerative diseases. Curr Med Chem. 15: 538–548, 2008.

Morrison RS, Kinoshita Y. The role of p53 in neuronal cell death. Cell Death Differ. 10: 868–879, 2000.

Paruchuri S, Sjölander A. Leukotriene D4 mediates survival and proliferation via separate but parallel pathways in the human intestinal epithelial cell line Int 407. J Biol Chem. 278: 45577–45585, 2003.

Pazdernik TL, Emerson MR, Cross R, Nelson SR, Samson FE. Soman-induced seizures: limbic activity, oxidative stress and neuroprotective proteins. J Appl Toxicol. 21: 87–94, 2001.

Pejchal J, Österreicher J, Kassa J, Tichý A, Mokrý J. Activation of mitogen activated protein kinase (MAPK) pathways after soman poisoning in rat cerebellar granule neurons. J Appl Toxicol. 28: 689–693, 2008.

Pejchal J, Osterreicher J, Kassa J, Tichy A, Micuda S, Sinkorova Z, Zarybnicka L. Soman poisoning alters p38 MAPK pathway in rat cerebellar Purkinje cells. J Appl Toxicol. 29: 338–345, 2009.

Remmele W, Stegner HE. Recommendation for uniform definition of an immunoreactive score (IRS) for immunohistochemical estrogen receptor detection (ER-ICA) in breast cancer tissue. Pathologe. 8: 138–140, 1987.

Rivard N, Boucher MJ, Asselin C, L'Allemain G. MAP kinase cascade is required for p27 downregulation and S phase entry in fibroblasts and epithelial cells. Am J Physiol. 277: 652–664, 1999.

Schuh RA, Lein PJ, Beckles RA, Jett DA. Noncholinesterase mechanisms of chlorpyrifos neurotoxicity: altered phosphorylation of Ca^{2+}/cAMP response element binding protein in cultured neurons. Toxicol Appl Pharmacol. 182: 176–185, 2002.

Shin HS, Lee HJ, Nishida M, Lee MS, Tamura R, Yamashita S, Matsuzawa Y, Lee IK, Koh GY. Betacellulin and amphiregulin induce up-regulation of cyclin D1 and DNA synthesis activity through differential signaling pathways in vascular smooth muscle cells. Circ Res. 93: 302–310, 2003.

Steinboeck F, Hubmann M, Bogusch A, Dorninger P, Lengheimer T, Heidenreich E. The relevance of oxidative stress and cytotoxic DNA lesions for spontaneous mutagenesis in non-replicating yeast cells. Mutat Res. 688: 47–52, 2010.

Takekawa M, Adachi M, Nakahata A, Nakayama I, Itoh F, Tsukuda H, Taya Y, Imai K. p53-inducible wip1 phosphatase mediates a negative feedback regulation of p38 MAPK-p53 signaling in response to UV radiation. EMBO J. 19: 6517–6526, 2000.

Tian JQ, Quaroni A. Involvement of p21(WAF1/Cip1) and p27(Kip1) in intestinal epithelial cell differentiation. Am J Physiol. 276: 1245–1258, 1999.

Wilson JW, Pritchard DM, Hickman JA, Potten CS. Radiation-induced p53 and p21WAF-1/CIP1 expression in the murine intestinal epithelium: apoptosis and cell cycle arrest. Am J Pathol. 153: 899–909, 1998.

Wittlinger M, Grabenbauer GG, Sprung CN, Sauer R, Distel LV. Time and dose-dependent activation of p53 serine 15 phosphorylation among cell lines with different radiation sensitivity. Int J Radiat Biol. 83: 245–257, 2007.